

# Insight into Rett syndrome: MeCP2 levels display tissue- and cell-specific differences and correlate with neuronal maturation

Mona D. Shahbazian<sup>1</sup>, Barbara Antalffy<sup>2</sup>, Dawna L. Armstrong<sup>2</sup> and Huda Y. Zoghbi<sup>1,3,4,\*</sup>

<sup>1</sup>Department of Molecular and Human Genetics, <sup>2</sup>Department of Pathology, <sup>3</sup>Department of Pediatrics and <sup>4</sup>Howard Hughes Medical Institute, Baylor College of Medicine, One Baylor Plaza, Houston, TX 77030, USA

Received August 26, 2001; Revised and Accepted November 10, 2001

Rett syndrome (RTT) is a neurodevelopmental disorder caused by mutations in the methyl-CpG-binding protein 2 (*MECP2*) gene. Previous data have shown that *MECP2* RNA is present in all mouse and human tissues tested, but the timing of expression and regional distribution have not been explored. We investigated the spatial and temporal distribution of the MeCP2 protein during mouse and human development. We found that in the adult mouse, MeCP2 is high in the brain, lung and spleen, lower in heart and kidney, and barely detectable in liver, stomach and small intestine. There was no obvious correlation between protein levels and RNA levels, suggesting that translation may be post-transcriptionally regulated by tissue-specific factors. The timing of MeCP2 expression in mouse and human correlated with the maturation of the central nervous system, with the ontogenetically older structures such as the spinal cord and brainstem becoming positive before newer structures such as the hippocampus and cerebral cortex. In the cortex, MeCP2 first appeared in the Cajal–Retzius cells, then in the neurons of the deeper, more mature cortical layers, and finally in the neurons of the more superficial layers. The MeCP2 protein was eventually present in a majority of neurons but was absent from glial cells. Our data suggest that MeCP2 may become abundant only once a neuron has reached a certain degree of maturity, and that this may explain some aspects of the RTT phenotype.

## INTRODUCTION

Rett syndrome (RTT) is a childhood neurological disorder characterized by an initial 6–18 month period of apparently normal development followed by an abrupt loss of learned language and motor skills (1). Purposeful hand movements, for instance, are replaced by incessant hand-wringing motions. Over a period of a few years, deceleration of head growth, gait apraxia and growth retardation become apparent. In addition, RTT patients may develop seizures, autistic behavior, scoliosis, prolonged corrected QT intervals and breathing irregularities such as hyperventilation and apnea (2,3). Mutations in the methyl-CpG-binding protein 2 (*MECP2*) gene have been identified in 70–90% of RTT patients, making this the major if not the only cause of RTT (4–9).

In order to understand RTT pathogenesis, both the function and location of the gene product, MeCP2, must be evaluated. MeCP2 is thought to function as a transcriptional repressor in methylated regions of DNA via two distinct domains, a methyl-CpG-binding domain (MBD) (10) and a transcriptional repression domain (TRD) (11). Many proteins have been shown to contain MBDs, but so far, MeCP2 is unique in its ability to bind to a single symmetrical pair of methyl-CpG dinucleotides (12). This *in vitro* binding capacity has been substantiated *in vivo* by the demonstration that the localization

of MeCP2 on the chromosomes parallels that of 5-methylcytosine, which is densest in heterochromatic regions but also present in euchromatin (12). The TRD of MeCP2 represses transcription through its interaction with the Sin3A complex containing histone deacetylase 1 (HDAC1) and HDAC2, which remodel the chromatin structure such that it becomes refractory to transcription (13,14).

The location of MeCP2 has been analyzed at the RNA level and has revealed the presence of three alternatively spliced *MECP2* transcripts (1.9, 7.5 and 10 kb) produced by differential polyadenylation [poly(A)] site usage (15–17). At least one of these transcripts is present in all human tissues, but the abundance varies between tissues (15). Whether the transcripts have different physiological roles is unknown. The half-lives of the 1.9 and 10 kb transcripts are similar, but the distinct 3'-untranslated regions of these two transcripts may have disparate effects on the translation efficiency (15). RNA *in situ* hybridization analysis in mice has shown that *Mecp2* is ubiquitous in embryos and is found in most neurons of the postnatal brain, but is higher in the olfactory bulb and hippocampus (16).

In light of its promiscuous binding to the chromosomes and indiscriminate expression pattern, MeCP2 would appear to be essential for the silencing of numerous genes in virtually every

\*To whom correspondence should be addressed at: Department of Molecular and Human Genetics, Baylor College of Medicine, One Baylor Plaza, Houston, TX 77030, USA. Tel: +1 713 798 6523; Fax: +1 713 798 8728; Email: hzoghbi@bcm.tmc.edu

tissue. However, this is difficult to reconcile with the relatively restricted pathology of RTT. In fact, deletion of the mouse *Mecp2* gene solely in neurons produces a similar phenotype to that seen with deletion of *Mecp2* in all cells (18), supporting the idea that, despite its hypothesized role as a global transcriptional repressor, MeCP2 function may be most critical in neurons. However, an essential role for MeCP2 outside the central nervous system (CNS) cannot be excluded, since the phenotype of the mice was analyzed primarily with regard to neuronal function, and more subtle deficiencies outside the CNS may have been overlooked.

Given the existence of multiple RNA transcripts that show tissue-specific distributions and the possibility that the various transcripts may be translated with different efficiencies, we reasoned that a precise determination of the localization of MeCP2 required analysis of the protein itself. Therefore, we studied the tissue-specific distribution of the MeCP2 protein in mice by immunoblot analysis and the spatial and temporal distribution in mouse and human brains by immunohistochemistry (IHC). We demonstrate that the MeCP2 protein is high in brain, lung and spleen, moderate in kidney and heart, and low in liver, stomach and small intestine. In the brain, MeCP2 expression was not detected in glial cells and was abundant in mature neurons. These data suggest that the delayed onset and other characteristics of RTT may be partially explained by the preferential function of MeCP2 in mature rather than immature neurons.

## RESULTS

To determine the regional distribution of MeCP2, we quantified its levels in lysates of various adult mouse tissues by immunoblot analysis and found that it was present at highest levels in brain, lung and spleen (Fig. 1A). Expression in the kidney and heart was 2–4-fold lower than in the brain, and levels in the liver, stomach and small intestine were barely detectable, at levels ranging from 7- to 19-fold lower than in the brain. These tissue-specific differences were consistent between two independent animals. We were interested in whether this variation in protein level could be explained by differential expression of the *Mecp2* transcripts. To address this issue, we tested the distribution of the RNA in mouse and human tissues. A ~10 and ~2 kb transcript were present at varying levels in most tissues (Fig. 1B and C). To analyze the correlation between protein and RNA levels, we focused on tissues tested by immunoblotting and compared MeCP2/GAPDH protein ratios to the *MECP2* (or *Mecp2*)/ $\alpha$ -tubulin RNA ratios. The quantification for the mouse tissues clearly demonstrates the discrepancy between protein and mRNA levels (Fig. 1D). Similar results were obtained from analysis of the human tissues (data not shown).

To evaluate the distribution of MeCP2 by IHC, we generated two antisera: one to an N-terminal peptide (MeCP2N15) and one to a C-terminal peptide (MeCP2C17) (Materials and Methods). Specificity of the resulting antisera was confirmed by immunoblot analysis of transfected cell lysates and mouse brain extracts. A ~74 kDa protein was recognized by both antisera (Fig. 2).

The expression of MeCP2 in mouse was followed by IHC at the following developmental stages: embryonic day 10.5 (E10.5), E11.5, E13.5, E14.5, E16.5, E17.5, E18.5, postnatal

day 10 (P10) and 7 weeks after birth. At E10.5, MeCP2 was weakly detected in only a few cells in the marginal zone of the developing brain. A greater number of cells in this area were positive around E11.5 and expression was also seen in the spinal cord, pons and medulla (Table 1). At E14.5, MeCP2 was present in the thalamus, caudate/putamen and cerebellum. In addition, from E14.5 through E16.5, strong immunoreactivity was detected in neurons occupying the deeper, more mature layers of the cerebral cortex, but was absent from the more superficial, immature cortical neurons below the mature Cajal–Retzius cells in the marginal zone (Fig. 3A–C). The hypothalamus, hippocampus and deep cerebellar nuclei were immunoreactive to MeCP2 beginning around E16.5. By E18.5, all of the cortical layers expressed MeCP2 protein, but expression continued to be higher in the deeper layers than in the more superficial layers (Fig. 3D–F). At this time, most neurons expressed MeCP2 protein and there were no obvious additional neurons positive through the adult age. MeCP2 was not detected by IHC in embryonic tissues outside of the brain, with the exception of the ganglion cells and inner nuclear layer of the retina, but in the adult animal, MeCP2 was present in other tissues that were positive by immunoblot, such as lung and heart (data not shown).

Notably, the subcellular distribution of MeCP2 changed during mouse development, starting as a primarily diffuse nuclear staining from E10.5, but becoming increasingly punctate through E16.5. For example, this difference can be seen upon comparison of the cerebral cortex at E11.5 and E16.5 (Fig. 4A and B) and the spinal cord at E13.5 and E17.5 (Fig. 4C and D). It has been previously shown that in transfected mouse cells, MeCP2 co-localizes with Hoechst-positive heterochromatic foci (19). The punctate staining we observed was coincident with nuclear domains revealed by the chromatin-binding hematoxylin stain, suggesting that after mouse E14.5, there is a refinement of MeCP2 localization to heterochromatic domains.

Although MeCP2 appeared to be preferentially expressed in mature neurons of the brain, we sought to confirm its presence in older neurons by analyzing a 19-week-old mouse brain by IHC. MeCP2 was detected in most regions of the brain (Fig. 5A–H). To substantiate this result, we measured MeCP2 levels in whole brain lysates of mice ranging from P0 to 28 weeks old. It was apparent that MeCP2 levels remained relatively uniform from birth through 28 weeks of age (Fig. 5J), further suggesting the importance of MeCP2 function in mature neurons. Interestingly, although MeCP2 was expressed in most adult neurons, its levels appeared higher in some cells than others. We investigated this by immunofluorescence and found, for instance, that in the cerebellum, expression was highest in the Golgi cells, lower in Purkinje and stellate cells, and extremely low in the granule cells (Fig. 5I).

We next asked whether the developmental distribution of MeCP2 observed in the mouse would hold true in the human brain. Analysis of MeCP2 immunoreactivity by IHC demonstrated that at 10 and 14 weeks gestation (wg), MeCP2 was present in multiple brainstem nuclei and the Cajal–Retzius cells of the cerebral cortex. Deeper cortical layers began to show weak immunoreactivity around 19 wg, at which time MeCP2 also appeared in the thalamus, caudate, substantia nigra, globus pallidus and at low levels in the hippocampus and cerebellum (data not shown). By 26 wg, two distinct populations of neurons in the cerebral cortex showed

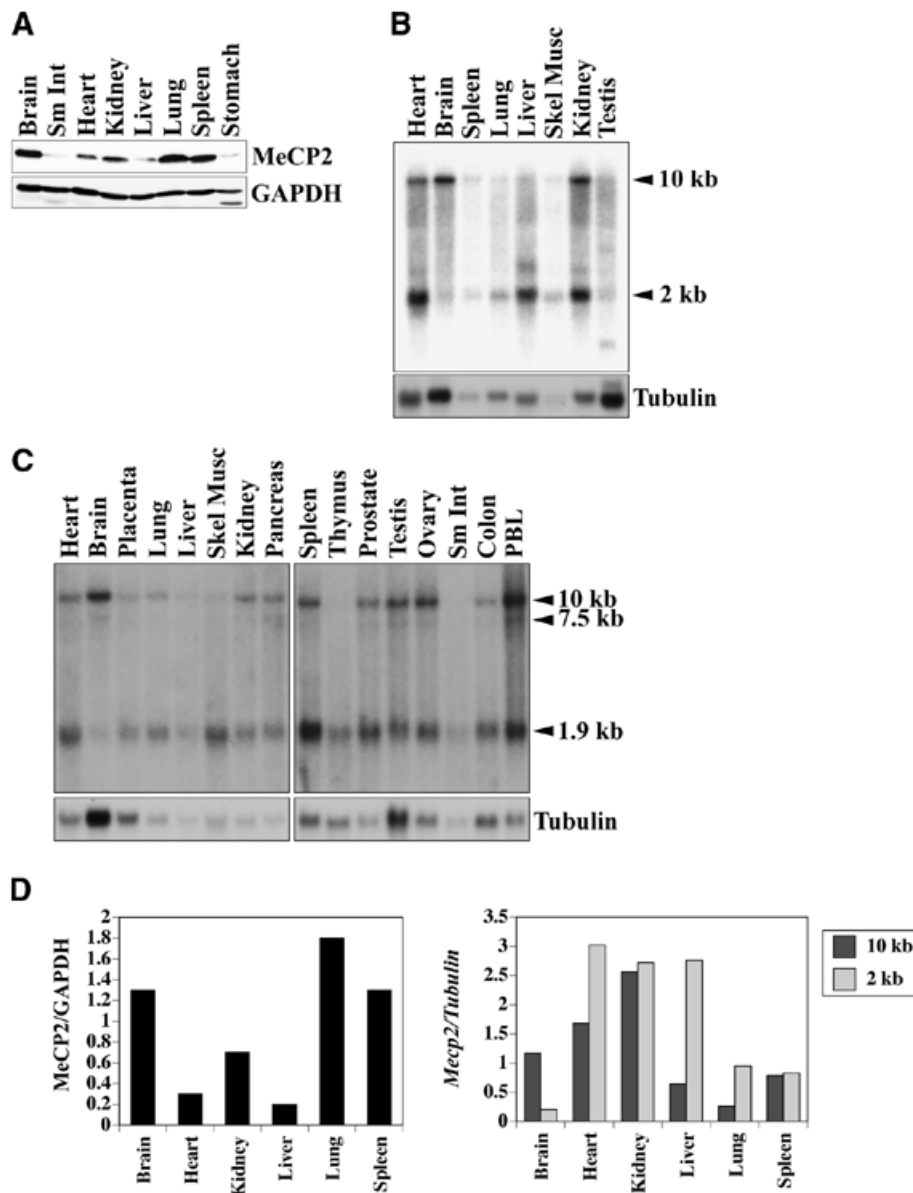


**Figure 1.** MeCP2 levels are highest in brain, lung and spleen. (A) Immunoblot analysis of tissues from a 9-week-old mouse shows that MeCP2 levels are highest in brain, lung and spleen, lower in kidney and heart, and barely detectable in small intestine, liver and stomach. Hybridization of northern blots of (B) mouse and (C) human tissues with a *MECP2* probe reveals that two major transcripts are differentially expressed. (D) To analyze the correlation between protein and RNA levels, we compared the MeCP2/GAPDH ratio (left) to the *MECP2*/ $\alpha$ -tubulin ratio (right). Graphs of the results for the mouse tissues are shown and reveal no correlation between protein and RNA levels. Abbreviations: Sm Int, small intestine; Skel Musc, skeletal muscle; PBL, peripheral blood leukocyte.

prominent MeCP2 expression: the Cajal–Retzius neurons and the deep cortical layers (Fig. 6A and B). Expression was also detected in the subplate neurons, ependyma, choroid plexus and spinal cord. Around 29 wg, the locus ceruleus, basis pontis and colliculi expressed MeCP2 (data not shown). With the exception of the putamen, which became positive around 35 wg, the remainder of the expansion in MeCP2 expression was confined to the cortex, showing a gradual increase from ~10% positive neurons at 26 wg to >80% around 10 years (Fig. 6B–D). In contrast, in areas such as the reticular formation of the brainstem, a similar percentage of neurons were positive at 35 wg

(>80%) and 10 years (~100%) (Fig. 6E and F). Similar to the mouse, the intensity of immunostaining varied among different populations of neurons. For example, in the cerebellum, the granule cells and Purkinje cells showed much lower MeCP2 levels than the Golgi and stellate cells (data not shown). In contrast to the mouse, some brain regions consistently showed weaker staining, particularly the putamen and hippocampus (data not shown). Another difference in MeCP2 staining between the mouse and human brain was that in human neurons, MeCP2 was diffusely nuclear at all ages examined, without any distinct punctate staining (Fig. 6).

**Table 1.** Expression of MeCP2 during mouse development<sup>a</sup>

Age	MZ	Deep	Super	Thal	Hypo	C/P	Hipp	Pons	Med	SC	Cer	DN
E10.5	tr	–	–	ND	ND	ND	ND	–	–	–	ND	ND
E11.5	+/-	–	–	ND	ND	ND	ND	+/-	+/-	+/-	ND	ND
E13.5	+	–	–	–	NT	+/-	ND	tr	tr	+/-	ND	ND
E14.5	+	+/-	–	+	–	+/-	NT	+/-	+/-	NT	+/-	NT
E16.5	+	+	–	+	tr	tr	+/-	tr	+	+/-	tr	tr
E17.5	+	+	–	+	tr	tr	+/-	+	+	tr	+	+
E18.5	+	+	+	+	+/-	+	+/-	+	+	+	+	+
P10	+	+	+	+	+	+	+	+	+	NT	+	+
7 weeks	+	+	+	+	+	+	+	+	+	NT	+	NT

<sup>a</sup>Expression levels: +, expression in a majority of neurons; +/-, expression in some neurons; tr, trace expression in some neurons; –, negligible expression; ND, structure not sufficiently developed; NT, structure not tested. Regions: MZ, marginal zone; Deep, deep cortical layers; Super, superficial cortical layers; Thal, thalamus; Hypo, hypothalamus; C/P, caudate/putamen; Hipp, hippocampus; Med, medulla; SC, spinal cord; Cer, cerebellum; DN, deep cerebellar nuclei.

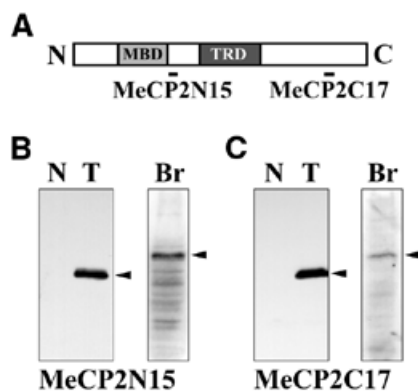


**Figure 2.** Specificity of antisera generated against MeCP2 peptides. (A) Diagram of the MeCP2 protein illustrating the positions of the MeCP2N15 and MeCP2C17 peptides. (B) Antiserum to MeCP2N15 recognizes a ~74 kDa protein (marked with arrow) in cells transfected with a *MECP2* cDNA (T) and in mouse brain extracts (Br) but not in non-transfected cells (N). (C) Antiserum to MeCP2C17 shows similar specificity.

MeCP2 expression in the mouse and human brains was detected in most neurons, but we were interested in whether the protein was present in glial cells. To address this, we performed double immunofluorescent labeling on the mouse brain with antibodies to MeCP2 and the glial marker, glial fibrillary acidic protein (GFAP). Several brain regions were analyzed but MeCP2 staining was never present in cells that were immunoreactive to GFAP (Fig. 7), suggesting that MeCP2 is absent from glia.

## DISCUSSION

Mutations in *MECP2* cause RTT, a neurological disorder characterized by loss of speech, abnormal movements, motor deficiencies and mental retardation. Early evidence based on RNA expression suggested that this repressor might be ubiquitous because *MECP2* transcripts were identified in all tissues examined and in both fetuses and adults. Several factors led us to question whether the distribution of the *MECP2* RNA was

representative of the protein distribution: (i) the discrepancy between the widespread expression pattern and the apparent neuronal specificity of RTT, (ii) the possibility of post-transcriptional regulation of the RNA, and (iii) the presence of multiple tissue-specific RNA transcripts that may serve different roles. Given these possibilities, we evaluated the spatial and temporal distribution of the MeCP2 protein.

We found that, in contrast to the previously described ubiquitous presence of the mouse *Mecp2* RNA (16), the protein was particularly abundant in brain, lung and spleen, less abundant in the kidney and heart, and almost negligible in the liver, stomach and small intestine. Quantification of the tissue distribution of RNA transcripts in mouse and human revealed that although the two differentially-polyadenylated transcripts varied in a tissue-specific manner, there was no correlation between these levels and protein levels. This finding suggests that *MECP2* transcripts are under post-transcriptional control and that this control is tissue specific rather than transcript specific. Although we expected MeCP2 levels to be high in the brain given the effect of *MECP2* mutations, the presence of substantial protein in lung and spleen, and moderate amounts in other tissues, suggests that the neuronal specificity of RTT is partially due to factors other than protein abundance. Possibilities include differences in levels of other methyl-CpG-binding transcriptional repressors or differential requirements for methylation-dependent silencing. It is possible that certain anomalies seen in RTT such as the prolonged corrected QT interval may result from MeCP2 dysfunction in the heart rather than the CNS, but this remains to be determined.

By studying the pattern of MeCP2 localization in the CNS of the mouse and human during development, we found that MeCP2 is preferentially abundant in mature neurons. For example, the timing of its appearance correlated with the ontogeny of the CNS. The spinal cord and brainstem develop first, whereas the cerebral hemispheres develop last (20). MeCP2 expression followed a similar time course in both mouse and human, with its early expression in the spinal cord and brainstem, and late expression in the hippocampus and cerebral cortex (Fig. 8). Furthermore, in the cerebral cortex,

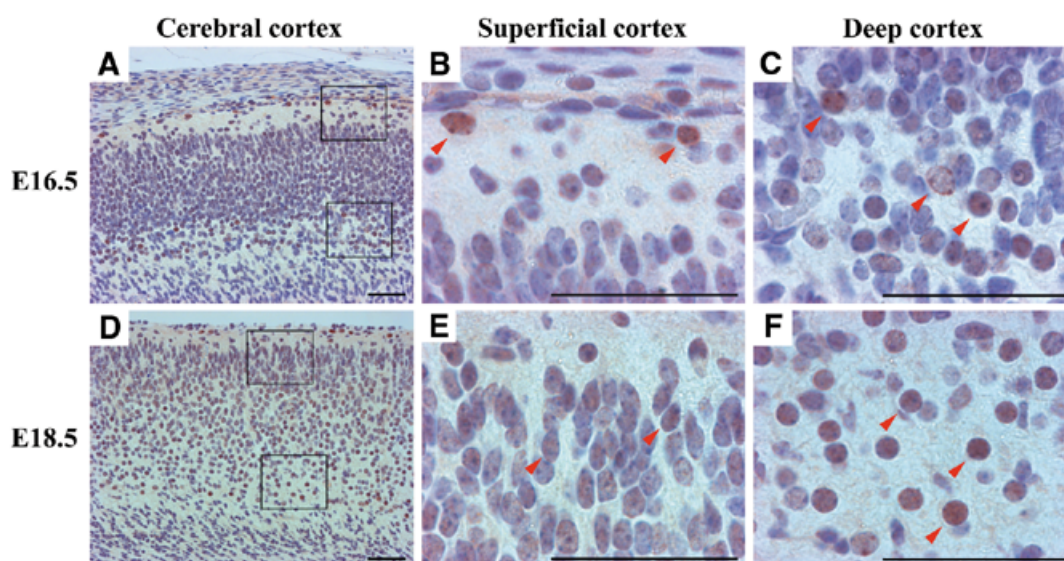


**Figure 3.** Higher MeCP2 expression in mature cortical neurons of the mouse brain. (A) At E16.5, MeCP2 expression is highest in the Cajal–Retzius neurons of the marginal zone [upper box, enlarged in (B)] and in the deepest, most mature layer of the cortex [lower box, enlarged in (C)]. Some examples of positive expression are indicated with red arrows. (D) MeCP2 is detectable in all layers of the cortex at E18.5, but is weaker in the superficial layers [upper box, enlarged in (E)] than the deep layers [lower box, enlarged in (F)]. Scale bars represent 50  $\mu$ m.

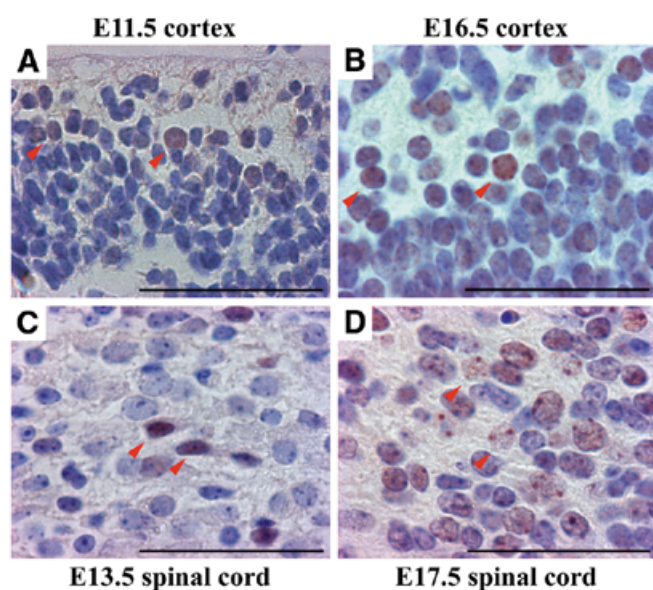


**Figure 4.** Developmental transition from a diffuse to a punctate nuclear staining pattern. (A) At E11.5, MeCP2 staining is diffuse in nuclei of cortical neurons, without any visible foci, whereas at E16.5, MeCP2 forms densely staining intranuclear foci (B). This is also seen in the spinal cord, where it is primarily diffuse at E13.5 (C) and primarily punctate at E17.5 (D). Scale bars represent 50  $\mu$ m.

where the developmental timing is well characterized, the order of MeCP2 expression followed that of neuronal maturation. All cortical neurons originate in the ventricular zone (VZ) and, after undergoing a mitotic phase, depart from the VZ and migrate towards the pial surface. The Cajal–Retzius neurons are born first and migrate into the marginal zone under the pial surface (21). Subsequent neurons migrate and form the cortical

plate below the marginal zone, with neurons occupying the deep layers of the cortical plate migrating first and subsequent neurons moving past these older neurons to form the more superficial cortical layers (20). We found that the Cajal–Retzius cells began to express MeCP2 first, followed by the deeper cortical layers and then the more superficial layers, consistent with the order of maturation. In the adult brain, MeCP2 was present in a majority of neurons, but not glia.

Although the general pattern of expression was similar in mouse and human, some differences were noted. For example, both species showed a gradual increase in the percentage of MeCP2-positive neurons, but in mouse, most of the increase was restricted to embryonic development, with most of the neurons that would subsequently express MeCP2 in the adult being positive by E18.5. In the human brain, although the number of MeCP2-positive neurons increased dramatically through gestation, the percentage of neurons expressing MeCP2 in the cortex continued to increase from birth through 10 years of age. Although the human tissue may be less reliable due to post-mortem protein degradation, the absence of MeCP2 in much of the cortex was consistent through multiple postnatal time points and in multiple samples before 10 years. Furthermore, in other areas such as the brainstem, the percentage of MeCP2-positive neurons remained constant. Therefore, we conclude that the differences in MeCP2 expression pattern between mouse and human are a result of species-specific differences. In light of the preferential expression of MeCP2 in mature neurons, we speculate that the delayed expression in the human cortex represents the extended period of developmental plasticity in humans, in which neurons have not achieved their fully differentiated state. Examples of experience-dependent plasticity are abundant for several areas of the cortex, including the visual, auditory and somatosensory cortices in humans and other animals (22). The cellular basis of this plasticity is thought to involve several aspects of neuronal



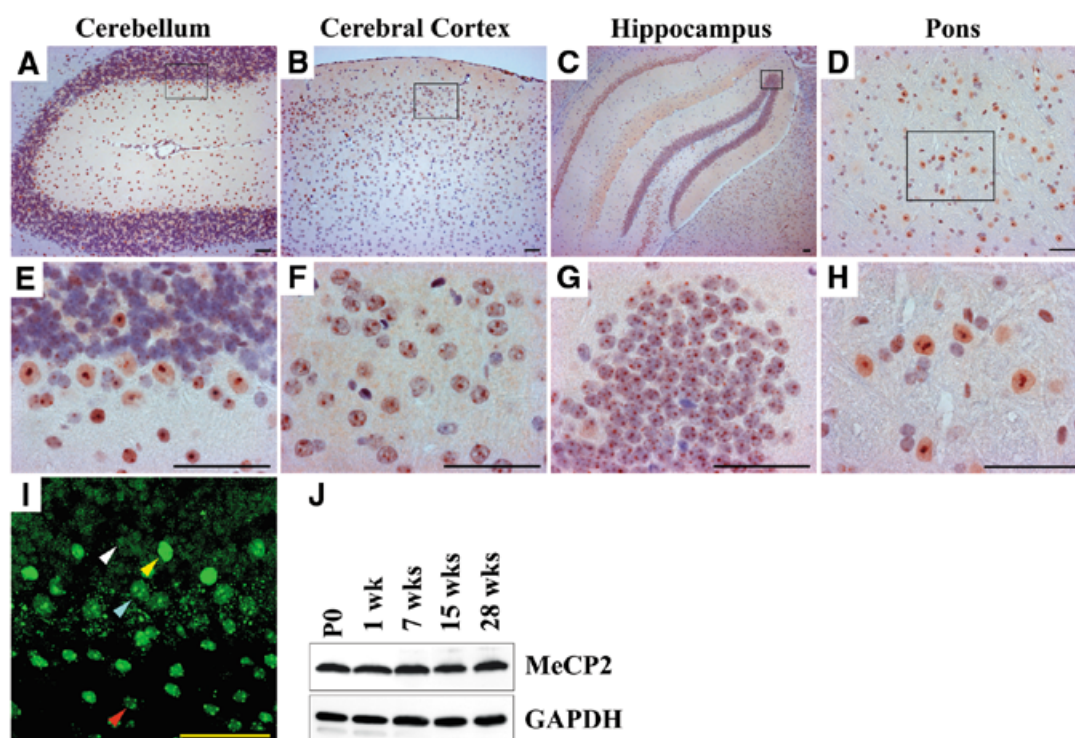


**Figure 5.** MeCP2 is expressed at high levels in the mature mouse brain. MeCP2 is expressed in most neurons of a 19-week-old mouse brain, including the cerebellum [(A), enlarged in (E)], cortex [(B), enlarged in (F)], hippocampus [(C), enlarged in (G)] and pons [(D), enlarged in (H)]. The cerebellum illustrates that the intensity of MeCP2 staining varied between cell types (I), with the Golgi cells (yellow arrow) showing highest levels, followed by the Purkinje cells (cyan arrow) and stellate cells (red arrow) at intermediate levels, and the granule cells (white arrow) at very low levels. Although the Golgi cells appear to have a diffuse staining pattern, a punctate distribution is seen at lower intensities (not shown). Measurement of MeCP2 levels in total brain lysates of mice at ages ranging from P0 to 28 weeks revealed that MeCP2 is present at high levels in the adult brain (J). Scale bars represent 50  $\mu$ m.

physiology, including synaptogenesis, myelination and neurotransmitter expression (23). Almost all species have a critical period during early development in which this process is most efficient (22). It has been shown that in humans, the time course of glucose utilization and synaptogenesis both show a dramatic increase between birth and 4 years of age, followed by a plateau until 10 years of age, and then a gradual decline during adolescence to the adult level (24). The timing of glucose metabolism has been shown to follow an ontogenetic order, with the neonatal period showing high levels in the brainstem, thalamus and cerebellar vermis, but low levels in most of the cerebral cortex until 8–12 months of age (24). The correlation in timing between MeCP2 expression, glucose utilization, synaptogenesis and experience-dependent plasticity in humans reinforces the idea that MeCP2 expression is delayed until neurons reach a certain stage of maturation, and further suggests that for at least some cortical neurons, this may be delayed until after the critical phase of experience-dependent plasticity.

Another notable difference in the expression of MeCP2 in mouse and human was on a subcellular level. Before mouse E16.5, MeCP2 was primarily diffuse in the nucleus, but from this time forth, it was mostly localized to discrete heterochromatic foci. In contrast, human MeCP2 was diffuse at all time points examined. This difference may be due to distinct patterns of heterochromatin localization in rodents and primates. Given that the change in distribution of mouse MeCP2 occurs at a distinct developmental stage, it is possible that the localization

of MeCP2 to its normal site of binding may be regulated by other cellular factors and that this may serve as a mechanism for controlling its silencing function.

The results described here, along with the previous observation that postnatal deletion of *Mecp2* in mouse neurons causes a phenotype that is delayed but otherwise similar to that produced by a null allele (18), points to a critical role for the MeCP2 transcriptional repressor in mature neurons. It may be that MeCP2 primarily represses genes that are important during neuronal development but which are detrimental for mature neurons. For example, developing neurons progress through a sequence of stages characterized by the expression of specific neurotransmitters and neuropeptides. The complement of signaling molecules expressed by the mature neuron may be entirely different from that during the embryonic stage (25–27). It could be that MeCP2 represses genes for some transmitters or peptides (or other factors) that are expressed only early in neuronal development. How MeCP2 might target specific genes is uncertain, but we envision a few possibilities: (i) The majority of MeCP2 binding sites, in regions of dense methylation, may be already saturated by other MBD-containing repressors, obviating a role for MeCP2. Other regions such as CpG islands may be more sparsely methylated, and since MeCP2 is the only member of the MBD family that has been shown to bind to a single symmetrical methyl-CpG dinucleotide pair, its function might be critical for the repression of genes controlled by these regions. (ii) During neuronal

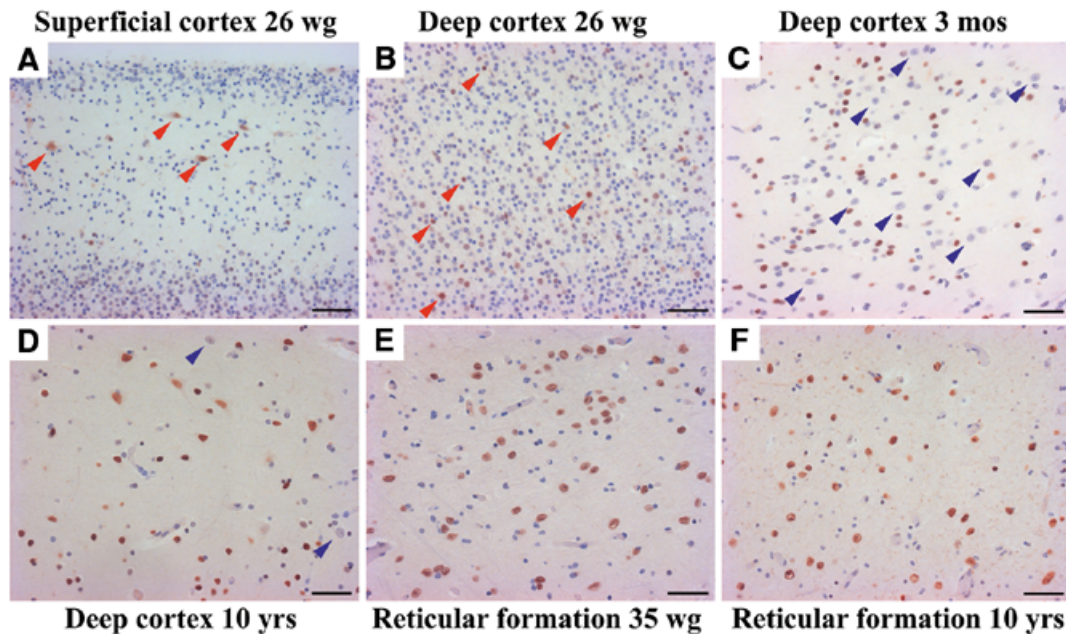


**Figure 6.** Delayed MeCP2 expression in human cortical neurons. (A) At 26 wg, the Cajal–Retzius neurons and (B) isolated cells in the deepest, most mature layer of the cortex express MeCP2. Examples of positive expression are indicated by red arrows. (C) At 3 months (mos), an increased number of deep cortical neurons show MeCP2 expression, but a large percentage of cells remain negative. Examples of negative cells are shown with blue arrows. At 10 years (yrs), only rare neurons demonstrate negligible MeCP2 expression (D). In contrast, the percentage of neurons expressing MeCP2 in the reticular formation of the brainstem is constant from 35 wg (E) to 10 years (F). Scale bars represent 50  $\mu$ m.

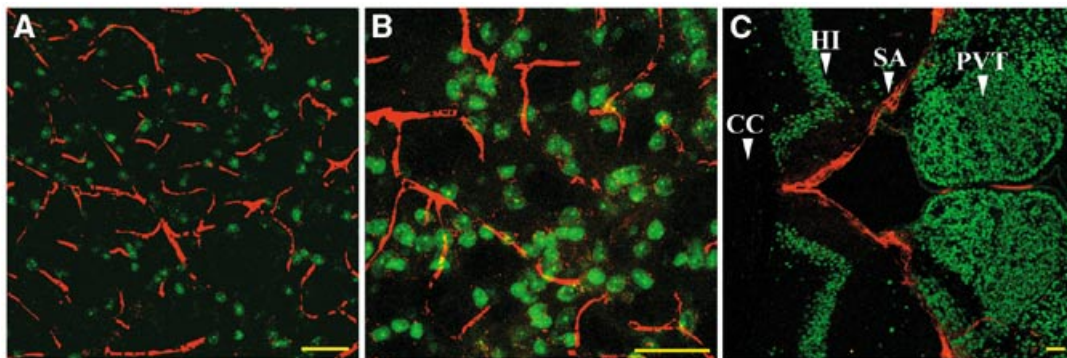


**Figure 7.** MeCP2- and GFAP-expressing cells are mutually exclusive. In the (A) pons [enlarged in (B)], MeCP2 staining (green) is absent from GFAP-positive (red) astrocytes. A section covering the corpus callosum (CC), hippocampus (HI) and periventricular thalamic nuclei (PVT) demonstrates the absence of MeCP2 from the subependymal astrocytes (SA). Scale bars represent 50  $\mu$ m.

maturation, certain genes may become methylated and it may be that only the MBD-containing protein that is most abundant or has the highest affinity for methylated DNA binds to these genes. The relative abundance of MBD family members in neurons is unknown, so it is possible that MeCP2 is more abundant than the other MBD-containing proteins in neurons. (iii) Certain DNA-binding proteins might guide MeCP2 to specific promoter sites to repress transcription of specific genes. This would be analogous to the recent finding that DNA methyltransferase 3a (Dnmt3a) serves as a co-repressor for RP58, a transcription silencer that binds to heterochromatin (28). We propose that one or more of these mechanisms

enables MeCP2 to repress the transcription of specific genes once a neuron has passed a critical phase of its development.

The prevalence of MeCP2 in mature neurons may have implications for at least some aspects of RTT. One of the intriguing features of the disease is that affected individuals typically have a 6–18 month period in which they acquire some motor and language skills. It is only after this period of normal development that these skills are lost. As there is no evidence of neuronal loss in RTT brains (29), the regression phase is best explained by a delayed onset of neuronal dysfunction. The findings that brain size (30), neuronal size (31) and dendritic branching (29) are reduced in RTT all suggest that neurons



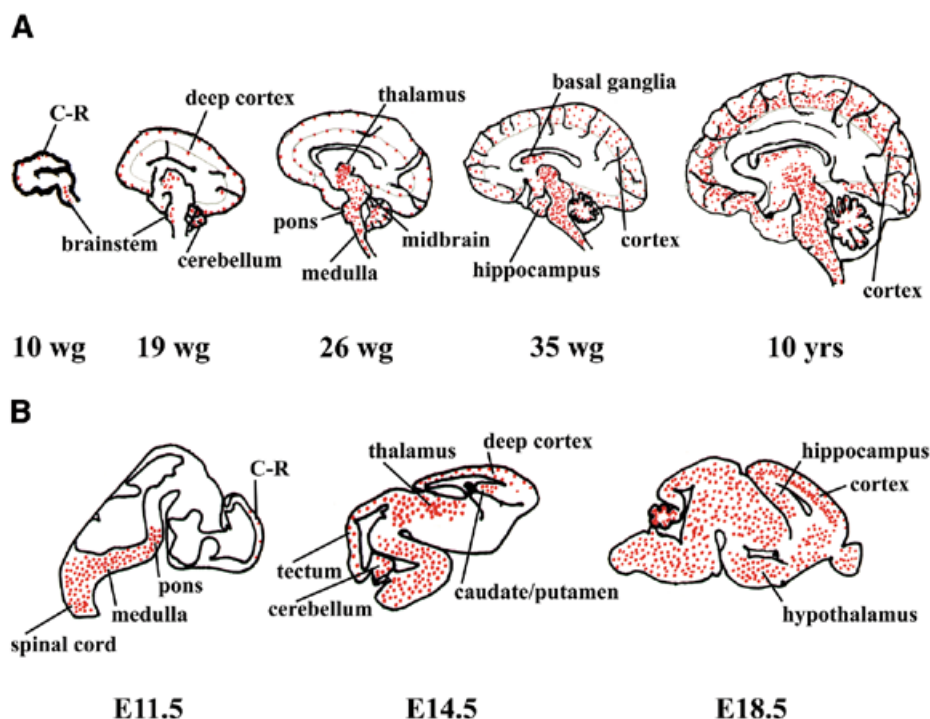


**Figure 8.** Schematic representation of the spatial and temporal distribution of MeCP2 during human and mouse development. The distribution of MeCP2 at selected ages during (A) human and (B) mouse CNS development is illustrated. The presence of MeCP2 is indicated with red dots. MeCP2 initially appears in the spinal cord, specific brainstem nuclei and in the Cajal–Retzius neurons (C-R) of the cerebral cortex. Expression is then seen in the midbrain, thalamus, cerebellum and deep cortical layers. MeCP2 appears later in the basal ganglia, hypothalamus, hippocampus and latest in the superficial cortical layers.

may be more immature in patients. It is conceivable that in the absence of proper MeCP2 function, neurons cannot advance to the fully mature state. Until now, the orderly, predictable progression of symptoms in RTT has had no known physiological correlate. Understanding the ontogeny of MeCP2 expression in the CNS may prove useful to exploring the pathogenesis of disorders caused by *MECP2* mutations.

## MATERIALS AND METHODS

### Northern blot hybridization

A mouse multiple tissue northern blot (Clontech) was hybridized with an 886 bp *Mbi*I genomic fragment containing a majority of the coding region of exon 4 using ExpressHyb hybridization solution (Clontech) and exposed to BioMax autoradiography film (Kodak). Signal intensities were quantified with a densitometer (Personal Densitometer SI, Molecular Dynamics) using ImageQuant Software (Molecular Dynamics). The blot was then stripped in boiling 0.5% SDS and hybridized with an  $\alpha$ -tubulin probe. The same procedure was followed for two human multiple tissue northern blots (Clontech) using the entire human *MECP2* cDNA as a probe.

### Antibody generation

An N-terminal peptide (MeCP2N15) and C-terminal peptide (MeCP2C17) were synthesized in the Protein Chemistry Core Laboratory (Baylor College of Medicine). The MeCP2N15

peptide represented amino acids 164–178 (SPSRREQKPP-KKPKS) of the human MeCP2 protein and the MeCP2C17 peptide represented amino acids 390–406 (PPEPESSEDPTSP-PEPQ). To both peptides, a C-terminal cysteine residue was added for conjugation to the carrier, keyhole limpet hemocyanin. Both conjugated peptides were injected into two rabbits to generate antisera (Bethyl Laboratories).

### Immunoblotting

Whole tissues were removed from mice after cervical dislocation, and homogenized in extraction buffer [100 mM Tris, pH 6.8, 2% SDS, 25 mM DTT, 5× protease inhibitor cocktail (Complete, Roche)] first with a tissue grinder (Dremel) and then with a dounce homogenizer. Total protein levels were quantified using a modified Bradford assay (Bio-Rad protein assay) and 100  $\mu$ g of protein was loaded onto an 8% SDS-polyacrylamide gel and separated by electrophoresis. Protein was transferred from the gel to a nitrocellulose membrane (Schleicher & Schuell). Blots were blocked in 5% blotting grade blocker non-fat dry milk (Bio-Rad) in Tris-buffered saline with 0.1% Tween-20 (TBS-T) for 1 h. Membranes were then incubated with MeCP2 antibody (Upstate Biotechnology) diluted 1:1000 or GAPDH antibody (Advanced Immuno-Chemical Inc.) diluted 1:20 000, in blocking solution for 1 h. The membrane was washed three times for 5 min with TBS-T and then incubated with blocking solution containing horseradish peroxidase-conjugated anti-rabbit IgG (Sigma) diluted 1:5000 for 45 min. Excess antibody was washed off with three



5 min TBS-T washes and the antibody conjugates were visualized by enhanced chemiluminescence (ECL, Amersham Life Science). Signals were quantified with a densitometer using ImageQuant Software.

### Immunohistochemistry

Seventeen human brains (ages 10 wg to 33 years) were obtained by informed consent from the Department of Pathology at Texas Children's Hospital and were investigated following Baylor College of Medicine Institutional Review Board approval. Mouse embryos and tissues were fixed either by transcardial perfusion with PBS-buffered 4% formaldehyde or by immersion in 10% formalin, washed and cut. Representative sections of cerebral cortex, basal ganglia, cerebellum, brain stem and spinal cord were dehydrated and impregnated with paraffin. Five micrometer sections were cut, mounted onto 'plus' slides, and antigen-retrieved in citric acid (pH 6.0) for three 5 min bursts of high microwave heat. Nuclear digestion was achieved with proteinase K. For the mouse tissues, anti-MeCP2 (Upstate Biotechnology) was used at a dilution of 1:100 for three nights at 4°C. For the human tissues, the MeCP2C17 crude serum was applied at a 1:300 dilution overnight at 4°C. Biotinylated anti-rabbit secondary antibodies were applied from the ABC-Elite kit (Vector Laboratories). Novared was used as chromagen.

### Immunofluorescence

Anesthetized mice were transcardially perfused with PBS followed by PBS-buffered 4% formaldehyde. Brains were removed and fixed overnight in PBS-buffered 4% formaldehyde at 4°C, followed by cryoprotection with a step-wise infiltration of 5–25% sucrose in 5% increments. Brains were cut coronally, embedded in optimal cutting temperature compound (O.C.T.; Tissue-Tek) and frozen. Forty-five micrometer sections were cut using a cryostat (Microm HM500) and rinsed free-floating in PBS. Sections were blocked for 1 h in 2% normal goat serum in PBS with 0.3% Triton X-100 (Roche) at 4°C. Rabbit polyclonal anti-MECP2 antibody (Upstate Biotechnology) was diluted 1:100 and mouse monoclonal anti-GFAP (Transduction Laboratories) was diluted 1:50 in blocking solution and incubated for 60 h at 4°C. After the sections were washed with TBS-T four times for 20 min, they were then incubated with Texas red-conjugated anti-mouse IgG (Vector Laboratories) and fluorescein-conjugated anti-rabbit IgG (Vector Laboratories) diluted 1:600 in blocking solution for 60 h at 4°C. Sections were then rinsed four times with TBS-T and mounted onto slides with mounting medium for fluorescence (Vector Laboratories) and viewed with a laser confocal microscope (Zeiss).

### ACKNOWLEDGEMENTS

The authors thank members of the Zoghbi Laboratory for critical comments on the manuscript. These studies were supported by an NIH predoctoral fellowship to M.D.S. (MH12555-01), NIH grant 1 PO1 HD40301 to H.Y.Z., and the Neuropathology core of the Baylor Mental Retardation Research Center (HD24064-14) and the International Rett Syndrome Association.

### REFERENCES

- Hagberg, B., Aicardi, J., Dias, K. and Ramos, O. (1983) A progressive syndrome of autism, dementia, ataxia, and loss of purposeful hand use in girls: Rett's syndrome: report of 35 cases. *Ann. Neurol.*, **14**, 471–479.
- The Rett Syndrome Diagnostic Criteria Work Group (1988) Diagnostic criteria for Rett syndrome. *Ann. Neurol.*, **23**, 425–428.
- Zoghbi, H.Y. and Francke, U. (2001) Rett syndrome. In Scriver, C.R., Beaudet, A.L., Sly, W.S. and Valle, D. (eds), *The Metabolic & Molecular Bases of Inherited Disease*. McGraw-Hill/Medical Publishing Division, New York, pp. 6329–6338.
- Shahbazian, M.D. and Zoghbi, H.Y. (2001) Molecular genetics of Rett syndrome and clinical spectrum of MECP2 mutations. *Curr. Opin. Neurol.*, **14**, 171–176.
- Nicolao, P., Carella, M., Giometto, B., Tavolato, B., Cattin, R., Giovannucci-Uzielli, M.L., Vacca, M., Regione, F.D., Piva, S., Bortoluzzi, S. and Gasparini, P. (2001) DHPLC analysis of the MECP2 gene in Italian Rett patients. *Hum. Mutat.*, **18**, 132–140.
- Vacca, M., Filippini, F., Budillon, A., Rossi, V., Mercadante, G., Manzati, E., Gualandi, F., Bigoni, S., Trabanelli, C., Pini, G. et al. (2001) Mutation analysis of the MECP2 gene in British and Italian Rett syndrome females. *J. Mol. Med.*, **78**, 648–655.
- Auranen, M., Vanhala, R., Vosman, M., Levander, M., Varilo, T., Hietala, R., Riikonen, R., Peltonen, L. and Jarvela, I. (2001) MECP2 gene analysis in classical Rett syndrome and in patients with Rett-like features. *Neurology*, **56**, 611–617.
- Laccone, F., Huppke, P., Hanefeld, F. and Meins, M. (2001) Mutation spectrum in patients with Rett syndrome in the German population: evidence of hot spot regions. *Hum. Mutat.*, **17**, 183–190.
- Bourdon, V., Philippe, C., Labrune, O., Amsellem, D., Arnould, C. and Jonveaux, P. (2001) A detailed analysis of the MECP2 gene: prevalence of recurrent mutations and gross DNA rearrangements in Rett syndrome patients. *Hum. Genet.*, **108**, 43–50.
- Nan, X., Meehan, R.R. and Bird, A. (1993) Dissection of the methyl-CpG binding domain from the chromosomal protein MeCP2. *Nucleic Acids Res.*, **21**, 4886–4892.
- Nan, X., Campoy, F.J. and Bird, A. (1997) MeCP2 is a transcriptional repressor with abundant binding sites in genomic chromatin. *Cell*, **88**, 471–481.
- Lewis, J.D., Meehan, R.R., Henzel, W.J., Maurer-Fogy, I., Jeppesen, P., Kleinf, F. and Bird, A. (1992) Purification, sequence, and cellular localization of a novel chromosomal protein that binds to methylated DNA. *Cell*, **69**, 905–914.
- Nan, X., Ng, H.H., Johnson, C.A., Laherty, C.D., Turner, B.M., Eisenman, R.N. and Bird, A. (1998) Transcriptional repression by the methyl-CpG-binding protein MeCP2 involves a histone deacetylase complex. *Nature*, **393**, 386–389.
- Jones, P.L., Veenstra, G.J., Wade, P.A., Vermaak, D., Kass, S.U., Landsberger, N., Strouboulis, J. and Wolffe, A.P. (1998) Methylated DNA and MeCP2 recruit histone deacetylase to repress transcription. *Nat. Genet.*, **19**, 187–191.
- Reichwald, K., Thiesen, J., Wiehe, T., Weitzel, J., Poustka, W.A., Rosenthal, A., Platzer, M., Stratling, W.H. and Kioschis, P. (2000) Comparative sequence analysis of the MECP2-locus in human and mouse reveals new transcribed regions. *Mamm. Genome*, **11**, 182–190.
- Coy, J.F., Sedlacek, Z., Bachner, D., Delius, H. and Poustka, A. (1999) A complex pattern of evolutionary conservation and alternative polyadenylation within the long 3'-untranslated region of the methyl-CpG-binding protein 2 gene (MeCP2) suggests a regulatory role in gene expression. *Hum. Mol. Genet.*, **8**, 1253–1262.
- D'Esposito, M., Quaderi, N.A., Ciccociola, A., Bruni, P., Esposito, T., D'Urso, M. and Brown, S.D. (1996) Isolation, physical mapping, and northern analysis of the X-linked human gene encoding methyl CpG-binding protein, MECP2. *Mamm. Genome*, **7**, 533–535.
- Chen, R.Z., Akbarian, S., Tudor, M. and Jaenisch, R. (2001) Deficiency of methyl-CpG binding protein-2 in CNS neurons results in a Rett-like phenotype in mice. *Nat. Genet.*, **27**, 327–331.
- Nan, X., Tate, P., Li, E. and Bird, A. (1996) DNA methylation specifies chromosomal localization of MeCP2. *Mol. Cell. Biol.*, **16**, 414–421.
- Jacobson, M. (1991) *Developmental Neurobiology*, 3rd edn. Plenum Press, New York.
- Marin-Padilla, M. (1998) Cajal–Retzius cells and the development of the neocortex. *Trends Neurosci.*, **21**, 64–71.

22. Berardi,N., Pizzorusso,T. and Maffei,L. (2000) Critical periods during sensory development. *Curr. Opin. Neurobiol.*, **10**, 138–145.
23. Insel,T.R. (1994) The development of brain and behavior. In Kupfer,D.J. and Bloom,F.E. (eds), *Psychopharmacology: The Fourth Generation of Progress (On-line edition)*. Raven Press, New York (<http://www.acnp.org/G4/GN401000066/>).
24. Chugani,H.T. (1998) A critical period of brain development: studies of cerebral glucose utilization with PET. *Prev. Med.*, **27**, 184–188.
25. Black,I.B. (1982) Stages of neurotransmitter development in autonomic neurons. *Science*, **215**, 1198–1204.
26. Jones,E.G. (1991) The development of the primate neocortex—an overview. In Mednick,S.A., Cannon,T.D., Barr,C.E. and Lyon,M. (eds), *Fetal Neural Development and Adult Schizophrenia*. Cambridge University Press, New York, pp. 40–65.
27. Armstrong,D.D., Assmann,S. and Kinney,H.C. (1999) Early developmental changes in the chemoarchitecture of the human inferior olive: a review. *J. Neuropathol. Exp. Neurol.*, **58**, 1–11.
28. Fuks,F., Burgers,W.A., Godin,N., Kasai,M. and Kouzarides,T. (2001) Dnmt3a binds deacetylases and is recruited by a sequence-specific repressor to silence transcription. *EMBO J.*, **20**, 2536–2544.
29. Armstrong,D., Dunn,J.K., Antalffy,B. and Trivedi,R. (1995) Selective dendritic alterations in the cortex of Rett syndrome. *J. Neuropathol. Exp. Neurol.*, **54**, 195–201.
30. Jellinger,K. and Seitelberger,F. (1986) Neuropathology of Rett syndrome. *Am. J. Med. Genet.*, **1** (suppl.), 259–288.
31. Bauman,M.L., Kemper,T.L. and Arin,D.M. (1995) Microscopic observations of the brain in Rett syndrome. *Neuropediatrics*, **26**, 105–108.